ARTICLE

Assignment of IVL-Methyl side chain of the ligand-free monomeric human MALT1 paracaspase-IgL$_3$ domain in solution

Xiao Han[1] · Maria Levkovets[2] · Dmitry Lesovoy[3] · Renhua Sun[1] · Johan Wallerstein[2] · Tatyana Sandalova[1] · Tatiana Agback[4] · Adnane Achour[1] · Peter Agback[4] · Vladislav Yu. Orekhov[2,5]

Abstract

Mucosa-associated lymphoid tissue protein 1 (MALT1) plays a key role in adaptive immune responses by modulating specific intracellular signalling pathways that control the development and proliferation of both T and B cells. Dysfunction of these pathways is coupled to the progress of highly aggressive lymphoma as well as to potential development of an array of different immune disorders. In contrast to other signalling mediators, MALT1 is not only activated through the formation of the CBM complex together with the proteins CARMA1 and Bcl10, but also by acting as a protease that cleaves multiple substrates to promote lymphocyte proliferation and survival via the NF-κB signalling pathway. Herein, we present the partial ^{1}H, ^{13}C Ile/Val/Leu-Methyl resonance assignment of the monomeric apo form of the paracaspase-IgL$_3$ domain of human MALT1. Our results provide a solid ground for future elucidation of both the three-dimensional structure and the dynamics of MALT1, key for adequate development of inhibitors, and a thorough molecular understanding of its function(s).

Keywords MALT1 · Paracaspase · ^{1}H · ^{13}C Ile · Val · Leu-Methyl resonance

Introduction

MALT1 has been identified as a key player in intracellular pathways that lead to the activation of the transcription factor NF-κB which ultimately controls the development and

Xiao Han and Maria Levkovets author have contributed equally to this work.

✉ Peter Agback
peter.agback@slu.se

✉ Vladislav Yu. Orekhov
vladislav.orekhov@nmr.gu.se

1 Science for Life Laboratory, Department of Medicine, Karolinska Institute, and, Division of Infectious Diseases, Karolinska University Hospital, 171 76 Stockholm, Sweden

2 Department of Chemistry and Molecular Biology, University of Gothenburg, Box 465, 40530 Gothenburg, Sweden

3 Department of Structural Biology, Shemyakin-Ovchinnikov, Institute of Bioorganic Chemistry RAS, Moscow, Russia 117997

4 Department of Molecular Sciences, Swedish University of Agricultural Sciences, Box 7015, 750 07 Uppsala, Sweden

5 Swedish NMR Centre, University of Gothenburg, Box 465, 40530 Gothenburg, Sweden

proliferation of T and B cells (Ruland et al. 2003; Ruefli-Brasse et al. 2003; Jaworski et al. 2014; Gewies et al. 2014; Bornancin et al. 2015; Juilland and Thome 2018; Schlauderer et al. 2018; Gehring et al. 2018; Hailfinger et al. 2009; Dunleavy and Wilson 2014; Lenz, 2015; Uren et al. 2000). The function of MALT1 is triggered upon activation of B- or T-cell receptors, as well as NK cells through interactions with Fc receptors (Rosebeck et al. 2011). Dysfunctions in these MALT1-directed pathways are coupled to the potential development of aggressive lymphomas with high resistance to current chemotherapies, as well as to the initiation of an array of immune disorders (Solsona et al. 2022) Full length MALT1 is composed of five domains (Hailfinger et al. 2009) including the N-terminal death domain (DD), two immunoglobulin-like domains (IgL$_1$ and IgL$_2$), the paracaspase or caspase-like domain (Casp) and a third immunoglobulin-like domain (IgL$_3$), followed by an unstructured C-terminal tail domain (Fig. 1A). The triggering of activating receptors from both innate and adaptive immune responses induces the formation of CARMA-BCL10-MALT1 (CBM) complexes (Ruland and Hartjes 2019). Indeed, CBM formation is pivotal for the adequate activation of the NF-κB transcription factor. The DD domain of MALT1 binds to the core of the BCL10 filament through interactions with the caspase
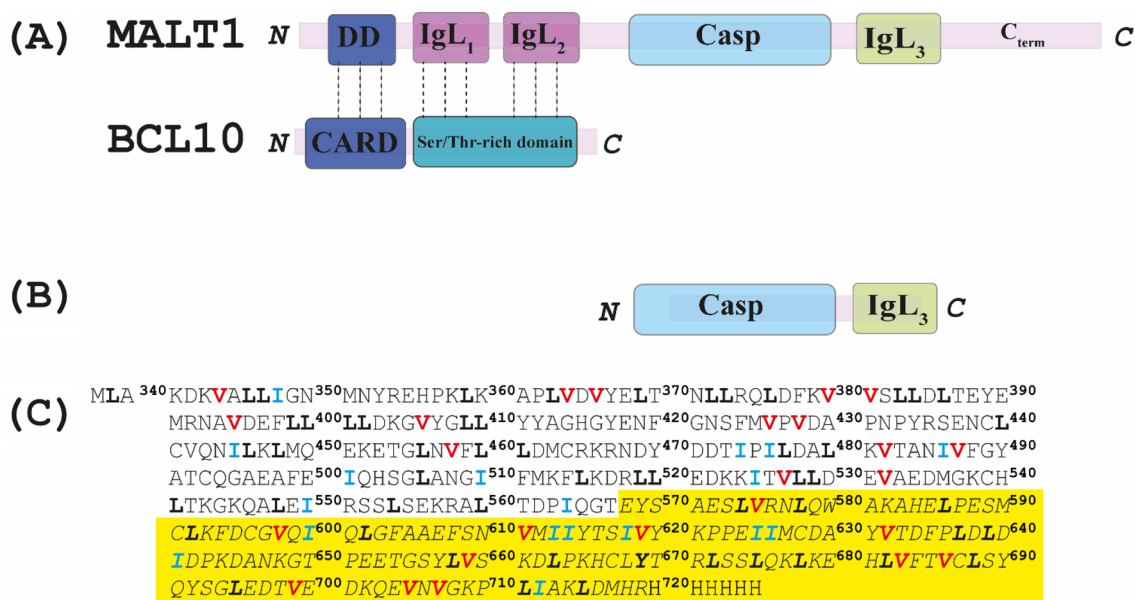
Fig. 1 Domain organization. **A** Schematic representation of the oligomer complex formed by MALT1 and BCL10. MALT1 comprises five domains including the N-terminal DEATH domain (DD), two immunoglobulin-like domains (IgL$_1$ and IgL$_2$), the caspase-like domain (Casp) and a third immunoglobulin-like domain (IgL$_3$) **B** Schematic representation of the MALT1(Casp-IgL$_3$)$_{338–719}$ self-folding unit that was used within the present study. **C** Sequence and numbering of human MALT1(Casp-IgL$_3$)$_{338–719}$ domains in which the IgL$_3$ domain is highlighted and typed in italic. The C-terminal his-tag is also depicted. The amino acids Ile, Leu and Val are labelled in blue, bold black and red, respectively

activation and recruitment domain (CARD) of BCL10 (Schlauderer et al. 2018), while additional interactions are also formed between the IgL$_1$ and IgL$_2$ domains of MALT1 and the Ser/Thr rich domain of BCL10 (Langel et al. 2008) (Fig. 1A). It should be noted that the C-terminal section of MALT1, which comprises the paracaspase and the IgL$_3$ domains, is most probably protruding out from the BCL10 filament, although its structure could not be detected due to high flexibility (Schlauderer et al. 2018) Thus, the molecular and dynamic bases underlying the potential allosteric modulation of the function of this section of MALT1 remain in our opinion unknown.

Importantly, it has been demonstrated that the regulating function of MALT1 on NF-κB can be exerted by at least two routes, one of which includes the protease activity acquired by MALT1 upon participating in the formation of the CBM complex (Che et al. 2004; Solsona et al. 2022; Rebeaud et al. 2008; Coornaert et al. 2008). However, it should be noted that MALT1 promotes a second route for NF-κB activation by acting as a scaffold when bound to BCL10, recruiting E3 ubiquitin ligases, such as TRAF6 and the linear ubiquitin chain assembly complex (LUBAC), which ultimately results in ubiquitination of BCL10 and MALT1 (Sun et al. 2004; Yang et al. 2014; Deng et al. 2000; Oeckinghaus et al. 2007). It has been previously demonstrated that activation of MALT1 requires the monoubiquitination of residue K644 on the surface of the IgL$_3$ domain (Fig. 1A) (Pelzer et al. 2013).

More recent data suggested that ubiquitination of the IgL$_3$ domain may induce conformational changes that could be allosterically communicated to the active site of the paracaspase domain of MALT1 (Schairer et al. 2020).

Crystal structures of individual MALT1 domains and combinations thereof in complex with allosteric ligands have been previously determined (Yu et al. 2011; Eitelhuber et al. 2015; Schlauderer et al. 2013). Furthermore, the recently developed AlfaFold prediction server provides an excellent source of reliably predicted three-dimensional structures of proteins and protein domains (Jumper et al. 2021), including human full-length MALT1 in monomeric form. However, although crystal structures provide crucial atomic-scale information about the three-dimensional fold of proteins as well as exquisite architectural details of e.g. catalytic sites, they still represent snapshots of energy minimized states and can thus seldom provide adequate information for e.g. establishing the dynamic bases underlying allosteric communication. Noteworthy, to the best of our knowledge, the three-dimensional structure of the apo monomeric form of the human MALT1(Casp-IgL$_3$)$_{338–719}$ in solution has remained missing and all available crystal structures of MALT1 are dimer (Yu et al. 2011; Wiesmann et al. 2012). In contrast, NMR spectroscopy can provide much more ample information about both domain and local conformational flexibilities. It has been previously demonstrated that the truncated version of MALT1 which comprises only the caspase-like

and the IgL$_3$ domains MALT1(Casp-IgL$_3$)$_{338–719}$ (Fig. 1B, C) retains an active fold (Wiesmann et al. 2012) and that it forms dimers that are functionally important (Hachmann et al. 2012; Wiesmann et al. 2012). Hence, we here focused our efforts on this part of MALT1. We have previously reported the almost complete ^{15}N/^{13}C/^{1}H backbone assignment of the apo form of the human MALT1 paracaspase region together with the third immunoglobulin-like (IgL$_3$) domain by high resolution NMR (Unnerstale et al. 2016). Here, we partially assigned the IVL-Methyl side chains of the ligand-free monomeric human MALT1 paracaspase-IgL$_3$ domain in solution.

Methods and experiments

Expression and purification of labelled MALT1(Casp-IgL$_3$)$_{338–719}$

The DNA sequence encoding for the caspase and IgL$_3$ domains of human MALT1, corresponding to residues 338–719 (Fig. 1C) and a C-terminal His6-tag was cloned into pET21b (Novagen). The MALT1$_{338–719}$-his construct was transformed into *Escherichia coli* strain T7 express competent cells and thereafter expressed in different isotopic labelling combinations in ^{1}/^{2}H, ^{15}N, ^{12}/^{13}C-labelled M9 medium. Chemicals for isotope labelling (ammonium chloride, ^{15}N (99%), D-glucose, ^{13}C (99%), deuterium oxide) were purchased from Cambridge Isotope Laboratories, Inc. Cells were cultivated at 37 °C and were induced at an OD$_{600}$ of approximately 0.8 for 16 h at 16 °C by addition of β-D-1-thiogalactopyranoside (IPTG) to 0.5 mM final concentration.

For the incorporation of methyl groups with the desired isotopic labelling pattern, alpha-keto acids were added as supplements to M9 medium and they served as biosynthetic precursors. MALT1(Casp-IgL$_3$)$_{338–719}$ was expressed in 1 L of D$_2$O M9 medium using 3 g/L of U-[^{13}C,^{2}H]-glucose (CIL, Andover, MA) as the main carbon source and 1 g/L of ^{15}NH$_4$Cl (CIL, Andover, MA) as the nitrogen source. One hour prior to induction, precursors were added to the growth medium as previously described (Tugarinov et al. 2006). For precursors, 70 mg/L alpha-ketobutyric acid, sodium salt (^{13}C4, 98%, 3,3-^{2}H, 98%) and 120 mg/L alpha-ketoisovaleric acid, sodium salt (1,2,3,4-^{13}C4,99%, 3, 4, 4, 4, -^{2}H 97%) (CIL, Andover, MA) were used. Bacterial growth was continued for 16 h at 16 °C and the cells were thereafter harvested by centrifugation.

Cells were resuspended in lysis buffer 20 mM TrisHCl (pH7.6), 150 mM NaCl, 2 mM DTT and lysed using ultrasonicator, followed by centrifugation at 40,000 g for 30 min to remove cell debris. The supernatant was collected and incubated with Ni^{2+} Sepharose 6 Fast Flow (GE Healthcare) for 1 h at 4 °C. The target protein was eluted with lysis buffer containing 200–500 mM imidazole. A Q-Sepharose HP column (GE Healthcare) was used to separate the monomeric MALT1(Casp-IgL$_3$)$_{338–719}$ protein from the dimer form. A final size exclusion chromatography (SEC) step using a HiLoad 16/600 Superdex 200 prep grade column (GE Healthcare) was performed, with running buffer 20 mM HEPES 7.4, 50 mM NaCl, 1 mM DTT. The final monomer MALT1(Casp-IgL$_3$)$_{338–719}$ protein sample was subsequently exchanged to a buffer (10 mM Tris 7.6, 50 mM NaCl, 2 mM TCEP, 0.002% NaN3) suitable for NMR experiments using gravity flow PD10 desalting columns (GE Healthcare). Final yields from a four litres M9 culture were approximately 8 mg of purified protein. Purified monomeric MALT1(Casp-IgL$_3$)$_{338–719}$-his was concentrated to at least 0.4 mM for NMR data acquisition.

NMR spectroscopy

NMR spectra were recorded at 298 K and 308 K on 700 MHz (Bruker AVANCE III) or on 800 MHz, 900 MHz (Bruker AVANCE III-HD) spectrometers equipped with cryo-enhanced 5 mm QXI, 3 mm TCI, and 3 mm TCI probes, respectively. 2D ^{1}H-^{15}N Best-TROSY-transverse relaxation optimized spectroscopy (TROSY) was used (Eletsky et al. 2001; Pervushin et al. 1997; Schulte-Herbruggen and Sorensen 2000). Three dimension (3D) Best-TROSY type HNCO and 3D HNCA experiments were collected using iterative non-uniformly sampling (NUS) (Favier and Brutscher 2011). Deuterium decoupling was applied in 3D Best-TROSY HNCA. The assignment of the ^{1}H, ^{13}C Methyl Val, Leu, Ile amino acids of MALT1(Casp-IgL$_3$)$_{338–719}$ was based on a set of 3D resonance experiments including HMCM(CGCB)CA and HMCM(CGCBCA)CO for Ile/Leu and HMCM(CB)CA for Val residues. The pulse programs were identical to hmcmcbcagpwg3d and hmcmcbcacogpwg3d in Bruker TopSpin3.6 except that methyl HMQC instead of HSQC and ^{2}H decoupling were applied (Tugarinov et al. 2014) and 1.8 ms IBurp1 pulse was used for selective inversion of CG2 of Ile.

Intramolecular amide- methyl, NH-CH$_3$, interactions were verified through observing cross peaks in 3D SOFAST (SF), ^{1}H–^{15}N TROSY NOESY experiments. Additional intramolecular Methyl-Methyl interactions were obtained from 4D ^{13}C,^{13}C-SF HMQC NOESY (Zwahlen et al. 1998) and 3D ^{1}H^{13}C^{13}C^{1}H-TOCSY(Kay et al. 1993) experiments.

The experimental parameters for acquisition in the 2D/3D/4D experiments are summarised in Table 1.

The 3D NUS methyl related experiments were processed using NMRpipe (Delaglio et al. 1995) and the IST algorithm in the mddnmr software (Kazimierczuk and Orekhov 2011; Mayzel et al. 2014). The decoupling of

Table 1 List of acquisition parameters used for NMR experiments

Experiments	Maximum evolution time, (ms)/ carrier frequency (ppm)/sweep width (ppm)			D1s	Scans	NUS points	NUS %	Time (h)
	F3	F2	F1					
^{1}H-^{15}N Best-TROSY[a,c]	9.4(^{1}H)/ 4.7/12	38.9(^{15}N)/ 118.0/36.0	–	0.8	4	–	–	1.0
3D Best-TROSY-HNCO[a,f]	79.9(^{1}H)/ 4.7/16.0	34.3(^{15}N)/ 118.0/36.0	19.9(^{13}C)/ 173.0/15.0	0.5	16	720	12	6.2
3D Best-TROSY – HNCA_2H[a,b]	106.5(^{1}H)/ 4.7/12.0	24.0(^{15}N)/ 118.0/36.0	42.4(^{13}C)/ 54.0/30.0	0.5	16	2400	13.4	32.4
3D ^{1}H–^{15}N SF-NOESY-TROSY[a]	79.9(^{1}H)/4.67/16.0	27.4(^{15}N)/118/36.0	28.4(^{1}H)/4.67/11.0	0.5	16	4600	23	68
4D ^{13}C,^{13}C-SF-HMQC NOESY-HMQC[c]	F481.0(^{1}H)/4.7/14.0	F3/F29.8(^{13}C)/ 17.0/18.0	F119.7(^{1}H)/4.7/1.8	0.7	8	5400	10.5	84
^{1}H^{13}C^{13}C^{1}H-TOCSY[g]	90.9(^{1}H)/4.67/1616.0	4.5(^{13}C)/39/80 36.0	22.7(^{1}H)/4.67/8 11.0	1.0	4	–	–	40
^{1}H-^{13}C HMQC[a,c]	94.6(^{1}H)/4.7/12.0	22.5(^{13}C)17.0/20.0	–	1.0	8	–	–	0.5
HMCM(CGCBCA) CO_2H[a,b,d,f]	91.8(^{1}H)/ 4.7/14.0 4.74.7	13.1(^{13}C)/16.0/16.0	28.9(^{13}C)/ 171.0/11.0	1.0	16	1612	60	37.4
HMCM(CGCB) CA_2H[a,b,d]	91.8(^{1}H)/ 4.7/14.0 4.74.7	13.1(^{13}C)/16.0/16.0	31.8(^{13}C)/ 39/20.0	1.0	16	1182	22	27
HMCM(CB)CA_2H[a,b,e]	91.8(^{1}H)/ 4.7/14.0 4.74.7	13.1(^{13}C)/16.0/16.0	31.8(^{13}C)/39.0/20.0	1.0	16	1720	32	38.4

[a]Experiments performed on an 800 MHz spectrometer

[b]Experiments performed with deuterium decoupling

[c]Experiments on 900 MHz spectrometer

[d]Optimized for Ile and Leu

[e]Optimized for Val

[f]T = 308 K

[g]Experiments performed on an 700 MHz spectrometer

the homonuclear one-bond ^{13}C$^\alpha$-^{13}C$^\beta$ scalar coupling in the HNCA, HMCM(CB)CA, and the HMCM(CGCB)CA experiments was performed by deconvolution (Kazimierczuk et al. 2020). The ^{1}H, ^{13}C and ^{15}N chemical shifts were referred to DSS-$_{d6}$. The ^{13}C and ^{15}N chemical shifts were referenced indirectly. The backbone chemical shifts of MALT1(Casp-IgL$_3$)$_{338-719}$, ^{1}HN, ^{15}N, ^{13}C$^\alpha$, ^{13}C$^\beta$ and ^{13}C′ nuclei, have been previously assigned by us (Unnerstale et al. 2016) using the Target Acquisition approach (Isaksson et al. 2013; Jaravine and Orekhov 2006; Jaravine et al. 2008), and can be found in the Biological Magnetic Resonance Data Bank (Ulrich et al. 2008) (http://www.bmrb.wisc.edu/) with the BMRB accession code 25,674. All analyses were performed manually in CcpNmr Analysis 3.0.4 (Vranken et al. 2005). For visualization of the results of Methyl's assignment on the MALT1(Casp-IgL$_3$)$_{338-719}$ model the UCSF Chimera package (Pettersen et al. 2004) was used. The model was created based on the crystal structure of MALT1 (PDB ID: 3V55) and adding missing loops according to the comparative protein modelling approach(Sali & Blundell 1993).

Extent of assignments and data deposition

Thorough knowledge of both backbone and side chain chemical shift nuclei is important for a complete description of the structural features of the human MALT1(Casp-IgL$_3$)$_{338-719}$ complex. We have previously reported the ^{15}N/^{13}C/^{1}H backbone assignment of the apo form of MALT1(Casp-IgL$_3$)$_{338-719}$ in solution (Unnerstale et al. 2016). Methyl-specific isotope labelling has been recently developed as a powerful tool to study the structure, dynamics and interactions of large proteins and protein complexes by solution-state NMR (Tugarinov et al. 2006; Rosenzweig and Kay 2014). Four large hydrophobic clusters assembled by methyl groups of Ile, Leu, Val amino acids could be distinguished in the structure of MALT1(Casp-IgL$_3$)$_{338-719}$ (Fig. 2). The first cluster (I) is located mainly in IgL$_3$ domain, while the second cluster (II) is localized between the IgL$_3$ and Casp (Fig. 2A). The third (III) and fourth (IV) clusters are structural parts of the Casp domain and are located on both side of beta sheets (Fig. 2B).

In this study, we focused on the assignment of the methyl resonances for the side chains of valine (Val), leucine (Leu)
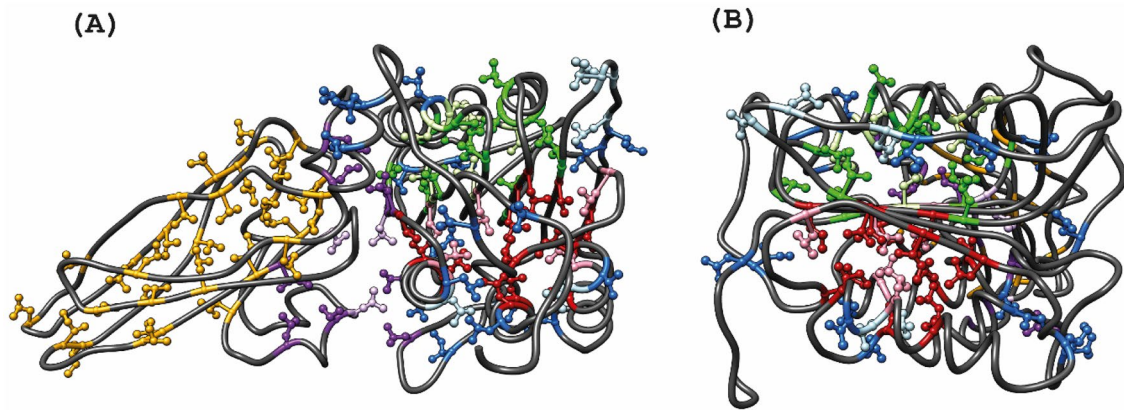
Fig. 2 Annotation of the Methyl groups assignment in the MALT1. **A** Four large hydrophobic clusters of methyl Ile, Val, Leu are coloured by: (I) yellow in IgL$_3$ domain, (II) violet, between IgL$_3$ and paracaspase domains, (III) and (IV) green and red for clusters located on both sides of the beta sheets in the paracaspase domain. **B** 90°-rotated projection of the paracaspase domain only showing (III) and (IV)

hydrophobic clusters located around the beta sheets. The methyls of Ile, Val and Leu residues that are lying outside of the hydrophobic cores of MALT1 are coloured in blue. The assigned methyl groups of the amino acids are marked by dark colours corresponding to the clusters and the unassigned residues are coloured in corresponding light colours

and isoleucine (Ile) amino acid residues in the human MALT1(Casp-IgL$_3$)$_{338-719}$ construct. The assignment of the ^{1}H and ^{13}C resonances of methyl group in NMR spectra of large proteins remains a challenge. We therefore used a combination of two highly efficient and complementing protocols. We started with the conventional approach, where the methyl resonances were connected to the known backbone assignments using methyl out-and-back experiments (Tugarinov et al. 2014). Then, the methyl assignments were validated and further expanded using the second approach based on Nuclear Oberhausen Effect (NOE) cross-peak data, peak residue type classification and a known 3D structure or a reliable structural model (Rossi et al. 2016; Pritišanac et al. 2019; Nerli et al. 2021).

Assignment of ^{1}H, ^{13}C resonances for methyl Ile, Leu and Val residues in human MALT1(Casp-IgL$_3$)$_{338-719}$ through Methyl -C$^\alpha$/ or C′ correlation

Our initial approach was based on sets of previously developed experiments (Tugarinov and Kay 2003), where interactions between ^{1}H/^{13}C labelled methyl groups of Ile, Val and Leu residues, and C$^\alpha$ or C′ nuclei in triple, ^{2}H, ^{13}C, ^{15}N, labelled MALT1(Casp-IgL$_3$)$_{338-719}$ protein were monitored. A higher resolution was achieved through NUS acquisition in indirect detection (Table 1). Combination of the previously obtained backbone assignment (Unnerstale et al. 2016) and chemical shifts for C$^\alpha$ and C' from the out-and-back methyl experiments (Table 1) allowed us to assign 10 (out of total 18) Ile, 12/108 Leu and 15 (of 52) Val methyl groups. The assignment at this stage was incomplete because

of the relatively low sensitivity of the methyl out-and-back 3D experiments, which lack cross-peaks for a number of methyl signals observed in 2D ^{1}H-^{13}C HMQC (Fig. 3). The apparent reason for this low sensitivity is fast relaxation of the ^{1}H and ^{13}C nuclei involved in the magnetization transfer. In addition, the Casp domain is apparently involved in a slow dynamic process leading to line broadening. The out-and-back HMCM(CGCBCA)CO_2H experiment performed at a higher temperature (308 K) showed higher sensitivity. However, we performed most of the experiments at 298 K, because MALT1(Casp-IgL$_3$)$_{338-719}$ is unstable at 308 K or higher temperatures. It should be noted that this type of experiment for large proteins usually shows best performance at high temperature, which therefore limits its application to temperature-stable proteins.

Assignment of ^{1}H, ^{13}C resonances for methyl Ile, Leu and Val residues in human MALT1(Casp-IgL$_3$)$_{338-719}$ based on NOEs contacts

As a next step, we combined backbone amide and side-chain methyl assigned above with NOEs obtained from NH-Methyl NOE in 3D (^{1}H-^{15}N) NOESY and Methyl-Methyl NOE interactions in 4D ^{13}C-^{13}C NOESY spectrum (Nerli et al. 2021) versus the available spatial structure of MALT1. Comparison of the observed NOE cross peaks and their intensities to the corresponding distances in the crystal structure of MALT1(Casp-IgL$_3$)$_{338-719}$ permitted additional assignment of the ^{1}H, ^{13}C methyl resonances. Pairs of geminal ^{13}C$^{\delta 1}$/^{13}C$^{\delta 2}$ and Val ^{13}C$^{\gamma 1}$/^{13}C$^{\gamma 2}$ resonances were verified

Fig. 3 Annotated ^{1}H,^{13}C-HMQC spectrum of monomeric human apo-MALT1(Casp-IgL$_3$)$_{338-719}$ Assignments of the cross peaks are depicted by numbers of the corresponding amino acid residues in the protein sequence. Numbers for Ile, Val and Leu are coloured in blue, red and black, respectively. The two insets enlarge the most crowded regions of the spectrum
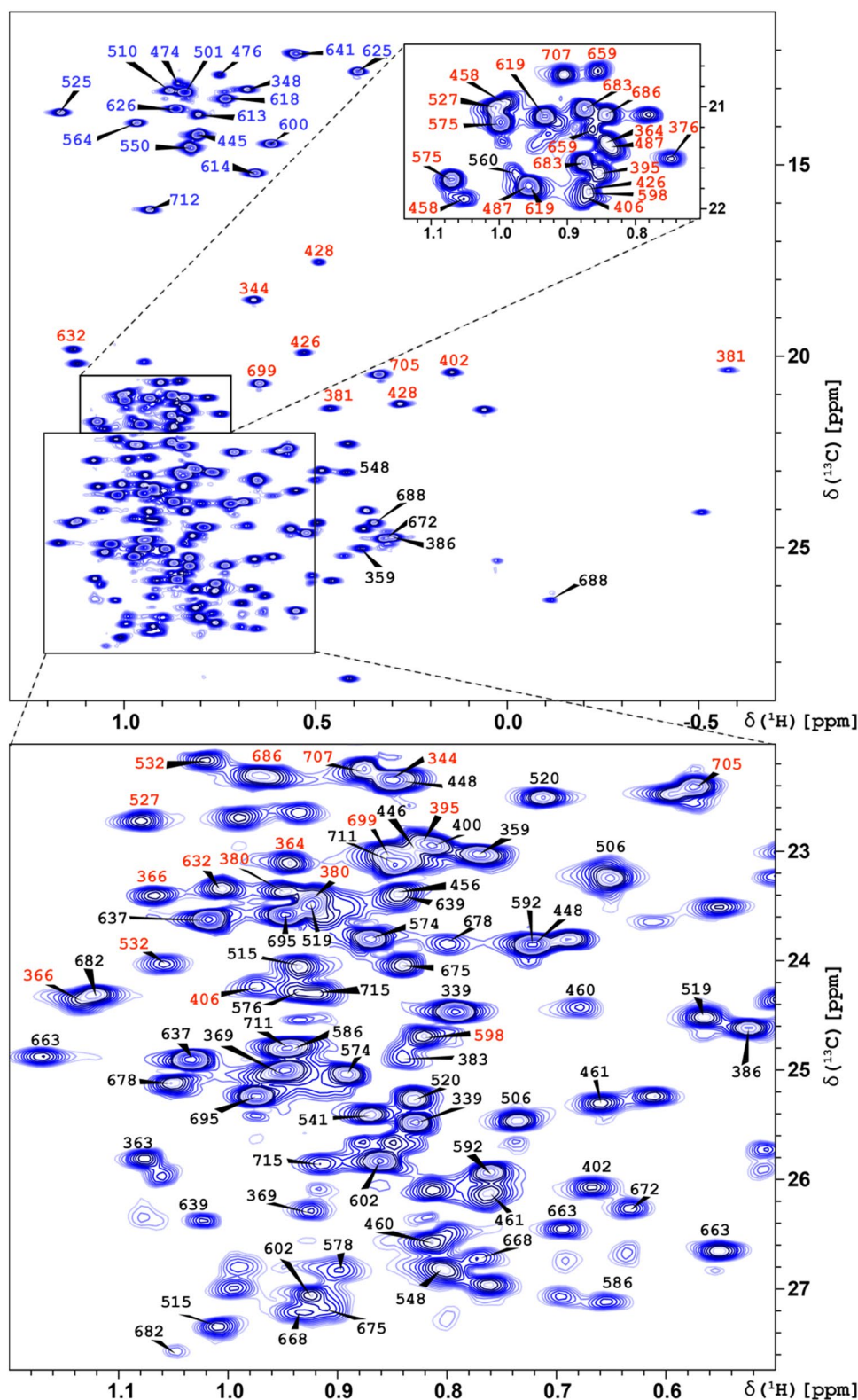
through Methyl-Methyl TOCSY interaction (Kay et al. 1993) in ^{1}H^{13}C^{13}C^{1}H-TOCSY experiment.

Figure 3 depicts the ^{1}H-^{13}C HMQC spectrum with the methyl assignment of MALT1(Casp-IgL$_3$)$_{338-719}$. Out of

a total of 98 ILV (61 in Casp and 37 in IgL$_3$) amino acid residues (only 1 methyl for Ile) we assigned 79 (44 for Casp and 35 for IgL$_3$): 88% of Val (13 in Casp and 10 in IgL$_3$, coloured in red in Fig. 3), 100% of Ile (10 in Casp

and 8 in IgL$_3$, coloured in blue in Fig. 3) and 70% of Leu (21 in Casp and 17 in IgL$_3$, coloured in black in Fig. 3). The majority of the assigned methyls are located in the IgL$_3$ domain and belong to the hydrophobic clusters I and II. Assignment of the remaining methyls in clusters (III) and (IV) was hindered by the incomplete backbone assignment, low sensitivity in the out-an-back spectra, as well as due to substantial overlap of several methyl signals of Leu residues. The methyl chemical shifts have been added to the Biological Magnetic Resonance Data Bank deposition 25,674. (Ulrich et al, 2008) (http://www.bmrb.wisc.edu/).

Conclusion

We present in this study the partial ^{1}H /^{13}C Ile/Leu/Val methyl resonance assignments for the apo form of human MALT1(Casp-IgL$_3$)$_{338–719}$. This assignment will play a crucial role in elucidation of MALT1(Casp-IgL$_3$)$_{338–719}$ structure, dynamics, and allosteric pathways as well as for mapping protein–protein and protein–ligand interaction sites.

Data availability The methyl chemical shifts have been added to the Biological Magnetic Resonance Data Bank deposition 25,674. (Ulrich et al., 2008) (http://www.bmrb.wisc.edu/).

Declarations

Conflict of interest The authors declare no competing interests for this work.

Ethical approval The work does not concern any ethical issues and did not involve any subjetcs.

Consent for publication All authors gave their consent for the publication.

References

Bornancin F, Renner F, Touil R, Sic H, Kolb Y, Touil-Allaoui I, Rush JS, Smith PA, Bigaud M, Junker-Walker U, Burkhart C, Dawson J, Niwa S, Katopodis A, Nuesslein-Hildesheim B, Weckbecker G, Zenke G, Kinzel B, Traggiai E, Brenner D, Brustle A, Paul MS, Zamurovic N, Mccoy KD, Rolink A, Regnier CH, Mak TW, Ohashi PS, Patel DD, Calzascia T (2015) Deficiency of MALT1 paracaspase activity results in unbalanced regulatory and effector t and b cell responses leading to multiorgan inflammation. J Immunol 194(8):3723–3734. https://doi.org/10.4049/jimmunol.1402254

Che TJ, You Y, Wang DH, Tanner MJ, Dixit VM, Lin X (2004) MALT1/paracaspase is a signaling component downstream of CARMA1 and mediates T cell receptor-induced NF-kappa B activation. J Biol Chem 279(16):15870–15876. https://doi.org/10.1074/jbc.M310599200

Coornaert B, Baens M, Heyninck K, Bekaert T, Haegman M, Staal J, Sun LJ, Chen ZJJ, Marynen P, Beyaert R (2008) T cell antigen receptor stimulation induces MALT1 paracaspase-mediated cleavage of the NF-kappa B inhibitor A20. Nat Immunol 9(3):263–271. https://doi.org/10.1038/ni1561

Delaglio F, Grzesiek S, Vuister GW, Zhu G, Pfeifer J, Bax A (1995) Nmrpipe—a multidimensional spectral processing system based on unix pipes. J Biomol NMR 6(3):277–293. https://doi.org/10.1007/Bf00197809

Deng L, Wang C, Spencer E, Yang L, Braun A, You J, Slaughter C, Pickart C, Chen ZJ (2000) Activation of the IkappaB kinase complex by TRAF6 requires a dimeric ubiquitin-conjugating enzyme complex and a unique polyubiquitin chain. Cell 103(2):351–361. https://doi.org/10.1016/s0092-8674(00)00126-4

Dunleavy K, Wilson WH (2014) Appropriate management of molecular subtypes of diffuse large B-cell lymphoma. Oncology-Ny 28(4):326–334

Eitelhuber AC, Vosyka O, Nagel D, Bognar M, Lenze D, Lammens K, Schlauderer F, Hlahla D, Hopfner KP, Lenz G, Hummel M, Verhelst SHL, Krappmann D (2015) Activity-based probes for detection of active MALT1 paracaspase in immune cells and lymphomas. Chem Biol 22(1):129–138. https://doi.org/10.1016/j.chembiol.2014.10.021

Eletsky A, Kienhofer A, Pervushin K (2001) TROSY NMR with partially deuterated proteins. J Biomol NMR 20(2):177–180. https://doi.org/10.1023/A:1011265430149

Favier A, Brutscher B (2011) Recovering lost magnetization: polarization enhancement in biomolecular NMR. J Biomol NMR 49(1):9–15. https://doi.org/10.1007/s10858-010-9461-5

Gehring T, Seeholzer T, Krappmann D (2018) BCL10-bridging cards to immune activation. Front Immunol 9:1539. https://doi.org/10.3389/fimmu.2018.01539

Gewies A, Gorka O, Bergmann H, Pechloff K, Petermann F, Jeltsch KM, Rudelius M, Kriegsmann M, Weichert W, Horsch M, Beckers J, Wurst W, Heikenwalder M, Korn T, Heissmeyer V, Ruland

J (2014) Uncoupling MALT1 threshold function from paracaspase activity results in destructive autoimmune inflammation. Cell Rep 9(4):1292–1305. https://doi.org/10.1016/j.celrep.2014.10.044

Hachmann J, Snipas SJ, van Raam BJ, Cancino EM, Houlihan EJ, Poreba M, Kasperkiewicz P, Drag M, Salvesen GS (2012) Mechanism and specificity of the human paracaspase MALT1. Biochem J 443:287–295. https://doi.org/10.1042/Bj20120035

Hailfinger S, Lenz G, Ngo V, Posvitz-Fejfar A, Rebeaud F, Guzzardi M, Penas EMM, Dierlamm J, Chan WC, Staudt LM, Thome M (2009) Essential role of MALT1 protease activity in activated B cell-like diffuse large B-cell lymphoma. P Natl Acad Sci USA 106(47):19946–19951. https://doi.org/10.1073/pnas.0907511106

Isaksson L, Mayzel M, Saline M, Pedersen A, Rosenlow J, Brutscher B, Karlsson BG, Orekhov VY (2013) highly efficient nmr assignment of intrinsically disordered proteins: application to B- and T cell receptor domains. PLoS ONE 8(5):e62947. https://doi.org/10.1371/journal.pone.0062947

Jaravine VA, Orekhov VY (2006) Targeted acquisition for real-time NMR spectroscopy. J Am Chem Soc 128(41):13421–13426. https://doi.org/10.1021/ja062146p

Jaravine VA, Zhuravleva AV, Permi P, Ibraghimov I, Orekhov VY (2008) Hyperdimensional NMR spectroscopy with nonlinear sampling. J Am Chem Soc 130(12):3927–3936. https://doi.org/10.1021/ja077282o

Jaworski M, Marsland BJ, Gehrig J, Held W, Favre S, Luther SA, Perroud M, Golshayan D, Gaide O, Thome M (2014) MALT1 protease inactivation efficiently dampens immune responses but causes spontaneous autoimmunity. EMBO J 33(23):2765–2781. https://doi.org/10.15252/embj.201488987

Juilland M, Thome M (2018) Holding all the CARDs: how MALT1 controls CARMA/CARD-dependent signaling. Front Immunol 9:1927. https://doi.org/10.3389/fimmu.2018.01927

Jumper J, Evans R, Pritzel A, Green T, Figurnov M, Ronneberger O, Tunyasuvunakool K, Bates R, Zidek A, Potapenko A, Bridgland A, Meyer C, Kohl SAA, Ballard AJ, Cowie A, Romera-Paredes B, Nikolov S, Jain R, Adler J, Back T, Petersen S, Reiman D, Clancy E, Zielinski M, Steinegger M, Pacholska M, Berghammer T, Bodenstein S, Silver D, Vinyals O, Senior AW, Kavukcuoglu K, Kohli P, Hassabis D (2021) Highly accurate protein structure prediction with alphafold. Nature. https://doi.org/10.1038/s41586-021-03819-2

Kay LE, Xu GY, Singer AU, Muhandiram DR, Formankay JD (1993) A gradient-enhanced HCCH-TOCSY experiment for recording side-chain 1H and 13C correlations in H 2O samples of proteins. J Magn Reson, Ser B 101(3):333–337. https://doi.org/10.1006/jmrb.1993.1053

Kazimierczuk K, Kasprzak P, Georgoulia PS, Matecko-Burmann I, Burmann BM, Isaksson L, Gustavsson E, Westenhoff S, Orekhov VY (2020) Resolution enhancement in NMR spectra by deconvolution with compressed sensing reconstruction. Chem Commun 56(93):14585–14588. https://doi.org/10.1039/d0cc06188c

Kazimierczuk K, Orekhov VY (2011) Accelerated NMR spectroscopy by using compressed sensing. Angew Chem Int Edit 50(24):5556–5559. https://doi.org/10.1002/anie.201100370

Langel FD, Jain NA, Rossman JS, Kingeter LM, Kashyap AK, Schaefer BC (2008) Multiple protein domains mediate interaction between Bcl10 and MALT1. J Biol Chem 283(47):32419–32431. https://doi.org/10.1074/jbc.M800670200

Lenz G (2015) Insights into the molecular pathogenesis of activated B-cell-like diffuse large B-cell lymphoma and Its therapeutic implications. Cancers 7(2):811–822. https://doi.org/10.3390/cancers7020812

Mayzel M, Kazimierczuk K, Orekhov VY (2014) The causality principle in the reconstruction of sparse NMR spectra. Chem Commun 50(64):8947–8950. https://doi.org/10.1039/c4cc03047h

Nerli S, De Paula VS, McShan AC, Sgourakis NG (2021) Backbone-independent NMR resonance assignments of methyl probes in large proteins. Nat Commun 12(1):691. https://doi.org/10.1038/s41467-021-20984-0

Oeckinghaus A, Wegener E, Welteke V, Ferch U, Arslan SC, Ruland J, Scheidereit C, Krappmann D (2007) Malt1 ubiquitination triggers NF-kappa B signaling upon T-cell activation. EMBO J 26(22):4634–4645. https://doi.org/10.1038/sj.emboj.7601897

Pelzer C, Cabalzar K, Wolf A, Gonzalez M, Lenz G, Thome M (2013) The protease activity of the paracaspase MALT1 is controlled by monoubiquitination. Nat Immunol 14(4):337–345. https://doi.org/10.1038/ni.2540

Pervushin K, Riek R, Wider G, Wuthrich K (1997) Attenuated T2 relaxation by mutual cancellation of dipole-dipole coupling and chemical shift anisotropy indicates an avenue to NMR structures of very large biological macromolecules in solution. Proc Natl Acad Sci U S A 94(23):12366–12371. https://doi.org/10.1073/pnas.94.23.12366

Pettersen EF, Goddard TD, Huang CC, Couch GS, Greenblatt DM, Meng EC, Ferrin TE (2004) UCSF chimera—a visualization system for exploratory research and analysis. J Comput Chem 25(13):1605–1612. https://doi.org/10.1002/jcc.20084

Pritišanac I, Würz JM, Alderson TR, Güntert P (2019) Automatic structure-based NMR methyl resonance assignment in large proteins. Nat Commun 10(1):1–12. https://doi.org/10.1038/s41467-019-12837-8

Rebeaud F, Hailfinger S, Posevitz-Fejfar A, Tapernoux M, Moser R, Rueda D, Gaide O, Guzzardi M, Iancu EM, Rufer N, Fasel N, Thome M (2008) The proteolytic activity of the paracaspase MALT1 is key in T cell activation. Nat Immunol 9(3):272–281. https://doi.org/10.1038/ni1568

Rosebeck S, Rehman AO, Lucas PC, McAllister-Lucas LM (2011) From MALT lymphoma to the CBM signalosome three decades of discovery. Cell Cycle 10(15):2485–2496. https://doi.org/10.4161/cc.10.15.16923

Rosenzweig R, Kay LE (2014) Bringing dynamic molecular machines into focus by methyl-TROSY NMR. Annu Rev Biochem 83:291–315. https://doi.org/10.1146/annurev-biochem-060713-035829

Rossi P, Xia Y, Khanra N, Veglia G, Kalodimos CG (2016) (15)N and (13)C- SOFAST-HMQC editing enhances 3D-NOESY sensitivity in highly deuterated, selectively [(1)H, (13)C]-labeled proteins. J Biomol NMR 66(4):259–271. https://doi.org/10.1007/s10858-016-0074-5

Ruefli-Brasse AA, French DM, Dixit VM (2003) Regulation of NF-kappaB-dependent lymphocyte activation and development by paracaspase. Science 302(5650):1581–1584. https://doi.org/10.1126/science.1090769

Ruland J, Duncan GS, Wakeham A, Mak TW (2003) Differential requirement for MALT1 in T and B cell antigen receptor signaling. Immunity 19(5):749–758. https://doi.org/10.1016/S1074-7613(03)00293-0

Ruland J, Hartjes L (2019) CARD-BCL-10-MALT1 signalling in protective and pathological immunity. Nat Rev Immunol 19(2):118–134. https://doi.org/10.1038/s41577-018-0087-2

Sali A, Blundell TL (1993) Comparative protein modelling by satisfaction of spatial restraints. J Mol Biol 234(3):779–815. https://doi.org/10.1006/jmbi.1993.1626

Schairer R, Hall G, Zhang M, Cowan R, Baravalle R, Muskett FW, Coombs PJ, Mpamhanga C, Hale LR, Saxty B, Iwaszkiewicz J, Decaillet C, Perroud M, Carr MD, Thome M (2020) Allosteric activation of MALT1 by its ubiquitin-binding Ig3 domain. Proc Natl Acad Sci U S A 117(6):3093–3102. https://doi.org/10.1073/pnas.1912681117

Schlauderer F, Lammens K, Nagel D, Vincendeau M, Eitelhuber AC, Verhelst SHL, Kling D, Chrusciel A, Ruland J, Krappmann D, Hopfner KP (2013) Structural analysis of phenothiazine

derivatives as allosteric inhibitors of the MALT1 paracaspase. Angew Chem Int Edit 52(39):10384–10387. https://doi.org/10.1002/anie.201304290

Schlauderer F, Seeholzer T, Desfosses A, Gehring T, Strauss M, Hopfner KP, Gutsche I, Krappmann D, Lammens K (2018) Molecular architecture and regulation of BCL10-MALT1 filaments. Nat Commun 9:4041. https://doi.org/10.1038/s41467-018-06573-8

Schulte-Herbrüggen T, Sorensen OW (2000) Clean TROSY: compensation for relaxation-induced artifacts. J Magn Reson 144(1):123–128. https://doi.org/10.1006/jmre.2000.2020

Solsona BG, Schmitt A, Schulze-Osthoff K, Hailfinger S (2022) The Paracaspase MALT1 in Cancer. Biomedicines 10(2):344. https://doi.org/10.3390/biomedicines10020344

Sun LJ, Deng L, Ea CK, Xia ZP, Chen ZJJ (2004) The TRAF6 ubiquitin ligase and TAK1 kinase mediate IKK activation by BCL10 and MALT1 in T lymphocytes. Mol Cell 14(3):289–301. https://doi.org/10.1016/S1097-2765(04)00236-9

Tugarinov V, Kanelis V, Kay LE (2006) Isotope labeling strategies for the study of high-molecular-weight proteins by solution NMR spectroscopy. Nat Protoc 1(2):749–754. https://doi.org/10.1038/nprot.2006.101

Tugarinov V, Kay LE (2003) Ile, Leu, and Val methyl assignments of the 723-residue malate synthase G using a new labeling strategy and novel NMR methods. J Am Chem Soc 125(45):13868–13878. https://doi.org/10.1021/ja030345s

Tugarinov V, Venditti V, Marius Clore G (2014) A NMR experiment for simultaneous correlations of valine and leucine/isoleucine methyls with carbonyl chemical shifts in proteins. J Biomol NMR 58(1):1–8. https://doi.org/10.1007/s10858-013-9803-1

Ulrich EL, Akutsu H, Doreleijers JF, Harano Y, Ioannidis YR, Lin J, Livny M, Mading S, Maziuk D, Miller Z, Nakatani E, Schulte CF, Tolmie DE, Wenger RK, Yao H, Markley JL (2008) BioMagResBank. Nucleic Acids Res 36:D402–D408. https://doi.org/10.1093/nar/gkm957

Unnerstale S, Nowakowski M, Baraznenok V, Stenberg G, Lindberg J, Mayzel M, Orekhov V, Agback T (2016) Backbone Assignment of the MALT1 Paracaspase by Solution NMR. PLoS ONE. https://doi.org/10.1371/journal.pone.0146496

Uren AG, O'Rourke K, Aravind L, Pisabarro MT, Seshagiri S, Koonin EV, Dixit VM (2000) Identification of paracaspases and metacaspases: Two ancient families of caspase-like proteins, one of which plays a key role in MALT lymphoma. Mol Cell 6(4):961–967. https://doi.org/10.1016/S1097-2765(00)00094-0

Vranken WF, Boucher W, Stevens TJ, Fogh RH, Pajon A, Llinas M, Ulrich EL, Markley JL, Ionides J, Laue ED (2005) The CCPN data model for NMR spectroscopy: development of a software pipeline. Proteins 59(4):687–696. https://doi.org/10.1002/prot.20449

Wiesmann C, Leder L, Blank J, Bernardi A, Melkko S, Decock A, D'Arcy A, Villard F, Erbel P, Hughes N, Freuler F, Nikolay R, Alves J, Bornancin F, Renatus M (2012) Structural determinants of MALT1 protease activity. J Mol Biol 419(1–2):4–21. https://doi.org/10.1016/j.jmb.2012.02.018

Yang YB, Schmitz R, Mitala J, Whiting A, Xiao WM, Ceribelli M, Wright GW, Zhao H, Yang YD, Xu WH, Rosenwald A, Ott G, Gascoyne RD, Connors JM, Rimsza LM, Campo E, Jaffe ES, Delabie J, Smeland EB, Braziel RM, Tubbs RR, Cook JR, Weisenburger DD, Chan WC, Wiestner A, Kruhlak MJ, Iwai K, Bernal F, Staudt LM (2014) Essential role of the linear ubiquitin chain assembly complex in lymphoma revealed by rare germline polymorphisms. Cancer Discov 4(4):480–493. https://doi.org/10.1158/2159-8290.Cd-13-0915

Yu JW, Jeffrey PD, Ha JY, Yang XL, Shi YG (2011) Crystal structure of the mucosa-associated lymphoid tissue lymphoma translocation 1 (MALT1) paracaspase region. P Natl Acad Sci USA 108(52):21004–21009. https://doi.org/10.1073/pnas.1111708108

Zwahlen C, Gardner KH, Sarma SP, Horita DA, Byrd RA, Kay LE (1998) An NMR experiment for measuring methyl-methyl NOEs in C-13-labeled proteins with high resolution. J Am Chem Soc 120(30):7617–7625. https://doi.org/10.1021/ja981205z